DMD Fast Forward. Published on November 5, 2013 as doi:10.1124/dmd.113.054783
This article has not been copyedited and formatted. The final version may differ from this version.

DMD #54783

Utility of oatp1a/1b-knockout and OATP1B1/3-humanized mice in the study of OATP-mediated pharmacokinetics and tissue distribution: case studies with pravastatin, atorvastatin, simvastatin, and carboxydichlorofluorescein.

J. William Higgins, Jing Q. Bao, Alice B. Ke, Jason R. Manro, John K. Fallon, Philip C. Smith, and Maciej J. Zamek-Gliszczynski

Drug Disposition, Lilly Research Laboratories, Indianapolis, IN (JWH, JQB, ABK, MJZG)

Global Statistical Sciences, Lilly Research Laboratories, Indianapolis, IN (JRM)

Eshelman School of Pharmacy, University of North Carolina, Chapel Hill, NC (JKF, PCS, MJZG)

DMD Fast Forward. Published on November 5, 2013 as DOI: 10.1124/dmd.113.054783
This article has not been copyedited and formatted. The final version may differ from this version.

DMD #54783

Running Title: OATP in drug pharmacokinetics and tissue distribution

Corresponding Author:

Maciej J. Zamek-Gliszczynski, Ph.D.

Lilly Corporate Center

Indianapolis, IN 46285, USA

Tel: 317-277-5664

Fax: 317-655-2863

E-mail: m_zamek-gliszczynski@lilly.com

Abstract: 248

Introduction: 749

Discussion: 1,491

References: 38

Number of Tables: 1

Number of Figures: 7

Abbreviations: OATP, organic anion transporting polypeptide; Kp tissue-to-blood/plasma concentration ratio

DMD Fast Forward. Published on November 5, 2013 as DOI: 10.1124/dmd.113.054783
This article has not been copyedited and formatted. The final version may differ from this version.

Abstract

Although OATP-mediated hepatic uptake is generally conserved between rodents and humans at a gross pharmacokinetic level, the presence of three major hepatic OATPs with broad overlap in substrate and inhibitor affinity, and absence of rodent-human orthologs, preclude clinical translation of single-gene knockout/knockin findings. At present, changes in pharmacokinetics and tissue distribution of pravastatin, atorvastatin, simvastatin, and carboxydichlorofluorescein were studied in oatp1a/1b-knockout mice lacking the three major hepatic oatp isoforms, and in knockout mice with liver-specific knockin of human OATP1B1 or OATP1B3. Relative to wild-type controls, oatp1a/1b-knockout mice exhibited 1.6-19 fold increased intravenous and 2.1-115 fold increased oral drug exposure, due to 33-75% decreased clearance, 14-60% decreased volume of distribution, and ≤74 fold increased oral bioavailability, with the magnitude of change depending on the contribution of oatp1a/1b to pharmacokinetics. Hepatic drug distribution was 4.2-196 fold lower in oatp1a/1b-knockout mice; distributional attenuation was less notable in kidney, brain, cardiac and skeletal muscle. Knockin of OATP1B1 or OATP1B3 partially restored control clearance, volume, and bioavailability values (24-142% increase, ≤47% increase, and ≤77% decrease versus knockout, respectively), such that knockin pharmacokinetic profiles were positioned between knockout and wild-type mice. Consistent with liver-specific humanization, only hepatic drug distribution was partially restored (1.3-6.5 fold increase versus knockout). Exposure and liver distribution changes in OATP1B1-humanized versus knockout mice predicted the clinical impact of OATP1B1 on oral exposure and contribution to human hepatic uptake of statins within 1.7 fold, but only after correcting for human/humanized mouse relative protein expression factor (OATP1B1 = 2.2, OATP1B3 = 0.30).

DMD Fast Forward. Published on November 5, 2013 as DOI: 10.1124/dmd.113.054783
This article has not been copyedited and formatted. The final version may differ from this version.

Introduction

Organic anion transporting polypeptides (OATPs) are uptake transporters for a variety of organic amphiphiles of all charges, including small molecule drugs (Niemi, 2007; Shitara et al., 2013). While OATPs are expressed in all tissues relevant to drug disposition, including intestine, kidney, and brain, hepatic OATPs have by far the greatest impact on drug pharmacokinetics (Giacomini et al., 2010; Iusuf et al., 2012b). Clinical inhibition of hepatic OATPs can elicit high-magnitude drug interactions (>5 fold increase in systemic exposure), in contrast to other drug transporters, whose inhibition generally poses a low risk (≤ 2 fold increase in exposure) (Giacomini et al., 2010). Further highlighting their pharmacokinetic importance, humans carrying the OATP1B1 521T>C polymorphism consistently exhibit increased exposure to substrate drugs with appreciable clearance via this mechanism (Giacomini et al., 2013).

Clinical drug interactions with hepatic OATPs are especially relevant to 3-hydroxy-3-methyglutaryl coenzyme-A reductase inhibitor “statin” drugs due to the potential for altered efficacy and toxicity (Neuvonen et al., 2006). Inhibition of hepatic uptake can markedly impair drug distribution to the liver, the site of pharmacological activity, while elevating systemic exposure, which increases the potential for myotoxicity. OATP hepatic uptake influences pharmacokinetics of even the statins ultimately eliminated by metabolism and/or biliary excretion, because uptake is the rate-determining step in removal of these drugs from circulation (Elsby et al., 2012; Shitara et al., 2013).

Although human hepatic OATPs (1B1, 1B3, 2B1) have no direct rodent orthologs (major: 1a1, 1a4, 1b2; minor: 2b1), most substrates and inhibitors are nonspecific and interact with multiple isoforms in each species (van Montfoort et al., 2003; Iusuf et al., 2012b; Zamek-Gliszczynski et al., 2012b). Total OATP hepatic uptake is conserved between rodents and

DMD Fast Forward. Published on November 5, 2013 as DOI: 10.1124/dmd.113.054783
This article has not been copyedited and formatted. The final version may differ from this version.

humans at a gross kinetic level, with generally good translation of overall apparent substrate or inhibitor affinity and collective impact of OATPs on pharmacokinetics (Badolo et al., 2010; Iusuf et al., 2012b).

Absence of direct rodent-human OATP orthologs precludes isoform-specific mechanistic extrapolation from rodents to humans (Iusuf et al., 2012b). Knockout models lacking a single murine oatp isoform and OATP humanized wild-type mice, where a single human isoform is added to the full complement of rodent oatps, have virtually no predictive utility (Chen et al., 2008; Zaher et al., 2008; van de Steeg et al., 2009). Oatp1b2-knockout mice exhibited increased systemic exposure to some drugs taken up into the liver by OATPs [rifamycin SV (3-6 fold), rifampin (≤2 fold)] but not other such drugs [cerivastatin, lovastatin, simvastatin] (Chen et al., 2008; Zaher et al., 2008). These hit-and-miss findings cannot be explained by compensatory changes in oatp1a1/1a4/2b1, which were not observed (Zaher et al., 2008). Instead these results are kinetically consistent with hepatic uptake by multiple OATP isoforms (van Montfoort et al., 2003; Iusuf et al., 2012b; Zamek-Gliszczynski et al., 2013). When the fraction transported by the knocked-out OATP is not sufficiently large (>50%), exposure will not be markedly (>2 fold) increased (Zamek-Gliszczynski et al., 2009; 2013). Oatp1b2 mediates ~50% and 67-83% of rifampin and rifamycin SV systemic clearance, respectively; however for the statins, Oatp1b2 contribution was too low (<50%) to be detected within the variability of a mouse study (Zamek-Gliszczynski et al., 2009; 2013). Likewise, knockin of human OATP1B1 into wild-type mice elicited only a 17% decrease in oral methotrexate exposure (van de Steeg et al., 2009). Adding OATP1B1 to a liver already containing the full complement of murine oatps, is expected to have little impact on drug pharmacokinetics. Not only are exposure changes in OATP-humanized

wild-type mice small and difficult to discern, clinical translation of these data is virtually impossible.

In contrast, oatp1a/1b gene cluster knockout mice lack the three major liver isoforms and are essentially devoid of hepatic oatp function (van de Steeg et al., 2010). Although these mice still express oatp2b1, which is important in the intestine, the pharmacokinetic importance of rodent hepatic oatp2b1 is negligible (van de Steeg et al., 2010; Iusuf et al., 2012a; 2012b; Shitara et al., 2013). These knockout mice are a powerful *in vivo* model to investigate if, and to what extent, collective OATP hepatic uptake impacts pharmacokinetics. Furthermore, the knockout mice are the appropriate background for liver-specific knockin of human OATPs due to the effective absence of competing murine hepatic oatp activity (van de Steeg et al., 2012). Thus at present, systemic pharmacokinetics and tissue distribution of pravastatin, atorvastatin, simvastatin, and carboxydiclorofluorescein were compared across wild-type, oatp1a/1b-knockout, OATP1B1- and OATP1B3-humanized mice in order to determine the impact of hepatic OATPs on pharmacokinetics, as well as to explore the clinical translation of humanized mouse findings.

Materials and Methods

Chemicals: 5-(and 6)-carboxy-2',7'-dichlorofluorescein was purchased from Sigma-Aldrich (St. Louis, MO). Pravastatin, atorvastatin, simvastatin lactone, and simvastatin acid were purchased from Toronto Research Chemicals (North York, ON). All other chemicals were of reagent grade and were readily available from commercial sources.

Animals: Age-matched Oatp1a/1b cluster-knockout, OATP1B1- or OATP1B3-knockin mice humanized on the Oatp1a/1b-knockout background, and wild-type FVB male mice were purchased from Taconic (Hudson, NY). Mice were between 8-10 weeks of age (22-34 g) at time of study. Mice were delivered to Covance (Greenfield, IN), where they were acclimated for at least 3 days prior to study initiation. The Institutional Animal Care and Use Committee at Covance approved all animal procedures.

In animal studies, carboxydichlorofluorescein intravenous dose levels were selected based on body surface area scaling of rat doses (Zamek-Gliszczynski et al., 2012). Statin dose levels were selected to reflect the high end of human exposure in wild-type mice (University of Washington Drug Interaction database; control human PK values). Pravastatin exposures were comparable to high-end of human values; atorvastatin and simvastatin exposures were an order of magnitude higher in wild-type mice. The higher murine atorvastatin and simvastatin concentrations are not expected to affect translation of PK findings based on accurate (within 1.5-1.7 fold) clinical translation of these data with respect to OATP1B1 (see Discussion).

Human Liver Procurement: The human liver tissue samples for transporter protein quantification were sourced from the Eli Lilly and Company liver bank, which is comprised of ethically-sourced livers obtained under protocols approved by the appropriate committees for the conduct of human research at the Medical College of Wisconsin (Milwaukee, WI), the Medical

College of Virginia (Richmond, VA), Indiana University School of Medicine (Indianapolis, IN) and University of Pittsburgh (Pittsburgh, PA). The panel of livers analyzed contained 5 healthy male donors ranging in age from 18-45 years, and 3 healthy female donors ranging in age from 35-77 years.

Carboxydichlorofluorescein IV PK and Liver Distribution:

Carboxydichlorofluorescein is a preclinical OATP/MRP probe, which is metabolically stable and cleared approximately equally by biliary urinary excretion; hepatobiliary disposition is transporter-mediated with OATP uptake, MRP3 sinusoidal and MRP2 canalicular excretion (Zamek-Gliszczynski et al., 2003; 2012a). At present, carboxydichlorofluorescein intravenous pharmacokinetics were studied in order to demonstrate expected alterations with a molecule that exhibits simple pharmacokinetic properties. Blood concentration-time course of carboxydichlorofluorescein was determined in mice over 6 hours following tail vein injection (10 mg/kg; 5 mL/kg; 20% captisol in 25 mM phosphate buffer, pH = 8). Blood spots were collected onto DBS cards (226 Bioanalysis Card; PerkinElmer, Greenville, SC) via tail bleeds at 0.08, 0.25, 0.5, 1, 1.5, 2, 3, 4, 5, 6 hours post dose, and livers were excised and frozen at 6 hours.

Pravastatin and Atorvastatin PK and Tissue Distribution: Blood concentration-time courses of the two drugs were determined in two separate intravenous/oral cross-over studies with a 3-day washout period between drug administration. Pravastatin was administered on Day 0 by tail vein injection (10 mg/kg; 2 mL/kg of 20% Captisol in 25 mM phosphate buffer, pH = 8), and on Day 3 by oral gavage (100 mg/kg; 10 mL/kg of 1% hydroxyethylcellulose, 0.25% polysorbate-80, 0.05% antifoam in water). In a separate study, atorvastatin was administered on Day 0 by tail vein injection (10 mg/kg; 5 mL/kg of 20% Captisol, 15% ethanol in 25 mM phosphate buffer, pH = 8), and on Day 3 by oral gavage (300 mg/kg; 10 mL/kg of 1%

DMD Fast Forward. Published on November 5, 2013 as DOI: 10.1124/dmd.113.054783
This article has not been copyedited and formatted. The final version may differ from this version.

hydroxyethylcellulose, 0.25% polysorbate-80, 0.05% antifoam in water). Blood spots were collected via tail bleeds at 0.08, 0.25, 0.5, 1, 1.5, 2, 3, 4, 5, 6 hours post dose; 6 hours post oral drug administration, livers, right kidneys, brains, hearts, and right quadriceps were collected and frozen.

Simvastatin Composite PK and Tissue Distribution: Simvastatin PK was determined differently from the other analytes in order to describe PK of both the lactone and acid forms, which requires plasma sampling with immediate acidification (Yang et al., 2005). Composite plasma concentration-time course of simvastatin lactone and acid was determined over 6 hours. Simvastatin lactone was administered by tail vein injection (10 mg/kg; 1 mL/kg of 25% dimethylacetamide, 15% ethanol, 1% propyleneglycol, 25% 2-pyrrolidone, 25% water) or by oral gavage (100 mg/kg; 10 mL/kg of 1% hydroxyethylcellulose, 0.25% polysorbate-80, 0.05% antifoam in water). Plasma samples were collected at 0.08, 0.25, 0.5, 1, 1.5, 2, 3, 4, 5, 6 hours post dose from two groups of mice, which were sampled at alternating time points, with the first four samples collected via retro-orbital bleeds and the final blood draw by cardiac puncture. All plasma samples were immediately acidified by addition of equal volume of 21% phosphoric acid to maintain pH ~ 4.5 in order to prevent *ex vivo* simvastatin lactone hydrolysis to the acid (Yang et al., 2005). Livers, right kidneys, brains, hearts, and right quadriceps were collected and frozen at the time of final blood sampling (5 or 6 hours post oral drug administration).

Bioanalysis: Carboxydichlorofluorescein, pravastatin, atorvastatin, simvastatin lactone and acid concentrations in relevant matrices [blood spots (3-mm punch), acidified plasma, and tissue homogenates] were quantified by LC-MS/MS. All samples were mixed with an organic internal standard solution to precipitate protein, centrifuged, and the resulting supernatants were directly analyzed. Analytes were separated using reverse-phase chromatography with gradient

DMD Fast Forward. Published on November 5, 2013 as DOI: 10.1124/dmd.113.054783
This article has not been copyedited and formatted. The final version may differ from this version.

elution and detected in negative or positive ion mode using selected reaction monitoring [Sciex API 4000 triple quadrupole mass spectrometer equipped with a TurboIonSpray interface (Applied Biosystems/MDS; Foster City, CA)]: carboxydichlorofluorescein, $[M-H]^-$ *m/z* 443.0 → 363.0; pravastatin, $[M-H]^-$ *m/z* 423.1 → 321.1; atorvastatin, $[M+H]^+$ *m/z* 560.1 → 440.1; simvastatin lactone, $[M+NH_4]^+$ *m/z* 436.3 → 285.3; simvastatin acid, $[M+H]^+$ *m/z* 437.3 → 303.3. The dynamic range of the assays was 1-5000 ng/mL in all matrices for all analytes, except for blood carboxydichlorofluorescein (50-500,000 ng/mL), blood pravastatin (1-10,000 ng/mL), blood and liver atorvastatin (25-500,000 ng/mL).

Targeted Quantitative Proteomic Analysis: Liver tissue samples from mouse or human (approx. 100 mg), prepared in duplicate, were homogenized in cold hypotonic buffer (10 mM Tris-HCl, pH 7.4, 10 mM NaCl, 0.15 mM $MgCl_2$) with 1.5 mM PMSF and protease inhibitor cocktail (Sigma, St. Louis, MO) with 2 ml buffer per 100 mg tissue, then allowed to swell for 30 min on ice. The samples were then homogenized again and centrifuged at 10K x g for 10 min at 4°C. The supernatant was transferred to a tube and centrifuges at 100K x 60 min at 4°C. The supernatant was discarded, then the pellet suspended in 0.2 mL PBS and stored at –80°C until later measured for protein content and analysis for OATP expression by targeted quantitative proteomics with LC-MS.

OATPs 1B1 and 1B3 were quantified in the hepatocyte membrane fractions by modification of a previously published targeted quantitative proteomic method (Fallon et al., 2013) and with guidance from similar methods published by others (Ohtsuki et al., 2011; Balogh et al., 2012; Ji et al., 2012). Methods development followed procedures previously outlined by Picotti et al. (2010). Stable isotope labeled proteotypic peptides, purchased from JPT (Acton, MA), were used as standards in each sample. Briefly, the membrane samples (50 µg of total

membrane protein) were solubilized in 1% sodium deoxycholate, denatured with heat, reduced with dithiothreitol and carbamidomethylated with iodoacetamide. Stable isotope labeled peptides were added and samples were digested overnight with trypsin (20:1 protein to trypsin ratio), the optimum digestion time having been determined during assay qualification. A liver membrane sample previously prepared and analyzed in our laboratory was used as a control between batches, all samples for the study being analyzed in two batches. Following digestion the reaction was stopped by addition of 10% trifluoroacetic acid, the volume added being 10 % of the total reaction volume. Following centrifugation at 10K rpm for 5 min to remove most deoxycholate, the supernatant was treated with solid phase extraction. The eluate was evaporated to dryness under vacuum and reconstituted in 50 µL modified mobile phase A (water/acetonitrile/formic acid 98/2/0.1; i.e. 2 % ACN) for analysis by nanoUPLC-MS/MS (selected/multiple reaction monitoring mode). Injection volume was 2 µL (4 % of the sample). The analytical instrumentation and chromatographic conditions employed were as previously described (nanoAcquity, BEH130 C18 column, AB Sciex QTRAP 5500) (Fallon et al., 2013). The stable isotope labeled peptides and MRMs employed in the final analyses are shown in supplemental Table 1.

Data Analysis: Noncompartmental pharmacokinetic parameters were calculated using Watson v. 7.4 (Thermo Scientific; Waltham, MA).

The tissue distribution data was analyzed using a one-way ANOVA model on the $\log_{10}$ transformed responses to test for differences among the mouse groups by compound and tissue. The PK parameters for pravastatin and atorvastatin were analyzed using a one-way ANOVA model; simvastatin PK parameters are point estimates based on composite PK curves, and are not amenable to significance testing. For PK parameters that are best compared as a difference (ex.

F, Tmax, CL), no data transformation was performed. For PK parameters that are compared as a ratio (ex. AUC, Cmax), the response data was transformed using the $\log_{10}$ transformation prior to analysis. The PK parameters for carboxydichlorofluorescein were analyzed with a mixed effect ANOVA model to combine the data from the two studies. Study was treated as a random effect and mouse group was treated as a fixed effect. All post-hoc t-tests for pre-specified contrasts of mouse groups were conducted using Fisher's least significant difference method. In those instances where the overall model was not statistically significant, the Bonferroni adjustment was used. Comparisons of OATP1B1 and OATP1B3 protein levels between humanized mouse and human livers were conducted using an unequal variance t-test.

Data are reported as mean ± SD. In all cases, $p < 0.05$ was considered significant.

Results

Carboxydichlorofluorescein intravenous pharmacokinetics are summarized in Figure 1 and Table 1. Systemic exposure was on average 2.6 fold higher in oatp1a/1b-knockout mice as a result of 43% decreased clearance and 55% lower volume. Knockin of OATP1B3 decreased exposure to levels comparable with wild type (2.6 fold decrease relative to knockouts), but the decrease was modest in OATP1B1-knockin mice (1.6 fold decrease versus knockouts). Knockin of OATP1B3 increased clearance and volume 41% and 24% relative to knockout mice, respectively, while OATP1B1 knockin did not markedly increase these parameters.

Carboxydichlorofluorescein biliary excretion accounts for approximately half of systemic clearance (Zamek-Gliszczynski et al., 2012a), thus reduced clearance and volume in oatp1a/1b-knockout mice are consistent with impaired hepatic uptake. Indeed, liver distribution was 37 fold decreased in oatp1a/1b knockout mice (Figure 1C), and was partially reconstituted by OATP1B3 knockin (6.5 fold increase versus knockout), but was only modestly increased in OATP1B1-knockin mice (2.4 fold higher than knockout).

Pravastatin pharmacokinetics are summarized in Figure 2 and Table 1. In oatp1a/1b-knockout mice, clearance was decreased 33% and volume was 21% lower. Conceptually consistent with both decreased clearance and volume, pravastatin systemic exposure following intravenous administration was on average 4.3 fold higher in oatp1a/1b-knockout mice. OATP1B1 knockin decreased intravenous exposure to levels comparable with wild type (4.6 fold decrease relative to knockouts), while knockin of OATP1B3 decreased exposure only slightly (15% decrease versus knockouts). Knockin of OATP1B1 increased clearance and volume 24% and 8% relative to knockout mice, respectively, but OATP1B3 knockin did not similarly increase these parameters. Following oral pravastatin administration, exposure and Cmax were 115 and

213 fold increased in oatp1a/1b-knockout mice, a change driven primarily by 74 fold increased oral bioavailability, and secondly, by the relatively minor decreases in clearance and volume. Tmax was shifted 3.1 fold earlier in the knockouts. OATP1B1 and OATP1B3 knockin modestly decreased oral drug exposure relative to the knockout background (AUC 45-58%, Cmax 67-88%), as a result of 10-48% decreased bioavailability, in addition to the decreases in clearance and volume.

Atorvastatin pharmacokinetics are summarized in Figure 3 and Table 1. Intravenous drug exposure was on average 19 fold increased in oatp1a/1b-knockout mice, due to 4.0 fold reduced clearance and 2.5 fold reduced volume of distribution. In OATP1B3- and OATP1B1-humanized mice, intravenous drug exposure was reduced 5.7 and 12 fold relative to the knockout background, respectively, as a result of both 2.2-2.4 fold increased clearance and 25-47% higher volume. Oral drug exposure was increased 2.9 fold in oatp1a/1b-knockout mice, but was partially attenuated by knockin of OATP1B1 (28%) or OATP1B3 (33%). Likewise, Cmax was 4.1 fold higher in knockout mice, but was decreased 23-27% in the humanized mice. Overall, oral bioavailability was comparable across mouse groups.

Simvastatin lactone composite pharmacokinetics are summarized in Figure 4 and Table 1. Intravenous exposure was on average increased 1.6 fold in oatp1a/1b-knockout mice as a result of both 39% reduction in clearance and 14% reduction in volume of distribution. In OATP1B3-knockin mice exposure was reduced 27% relative to knockouts, due to 37% increase in clearance but with no change in volume. Intravenous exposure was not decreased by knockin of OATP1B1, and decreases in clearance or volume were not observed. Oral exposure was increased 2.1 fold in oatp1a/1b-knockout mice, consistent with 31% increased bioavailability, as well as reduced clearance and volume. Relative to the knockout background, OATP1B1 and

OATP1B3 knockin decreased oral exposure 2.9 and 1.9 fold due to 3.4 and 1.4 fold decreased bioavailability, respectively, as well as increased clearance in OATP1B3-knockin mice.

Simvastatin acid composite pharmacokinetics following intravenous and oral administration of simvastatin lactone are summarized in Figure 5 and Table 1. Intravenous exposure was on average 1.8 fold increased in oatp1a/1b-knockout mice. Although clearance of the acid was not measured, this finding is consistent with 42% reduced total (acid + lactone) simvastatin clearance. Knockin of OATP1B3 reduced exposure 29% relative to the knockout background, and increased total simvastatin clearance 38%. Knockin of OATP1B1 did not reduce simvastatin acid exposure or increase total simvastatin clearance. Simvastatin acid oral exposure was 3.2 fold greater in oatp1a/1b-knockout animals. Although bioavailability of the acid was not measured, this finding is consistent with 52% increased total simvastatin (acid + lactone) bioavailability, as well as reduced total simvastatin clearance. Knockin of OATP1B1 reduced oral exposure and total simvastatin oral bioavailability 4.3 fold; however, knockin of OATP1B3 did not reduce either parameter.

Statin tissue distribution In oatp1a/1b-knockout mice, liver tissue-to-blood/plasma concentration ratio (Kp) of pravastatin, atorvastatin, and total simvastatin was on average decreased relative to wild type 196, 6.8, and 4.2 fold, respectively,. Knockin of OATP1B1 partially restored hepatic distribution (2.5, 1.2, 1.2 fold increase vs. knockout), as did knockin of OATP1B3 (5.7, 1.3, 1.6 fold increase vs. knockout) for pravastatin, atorvastatin, and total simvastatin, respectively. Atorvastatin and simvastatin renal tissue distribution was decreased 1.4-2.9 fold in knockout and knockin mice relative to wild type. In contrast, pravastatin kidney distribution was surprisingly increased 76 fold in oatp1a/1b-knockout mice, an effect which was 5.2 and 13 fold attenuated by knockin of OATP1B1 and OATP1B3, respectively. Brain

distribution was decreased in all knockout and knockin mice: 6.3-11, 1.3-1.4, and 3.0-4.2 fold for pravastatin, atorvastatin, and simvastatin, respectively. Cardiac and skeletal muscle distribution of pravastatin was inconsistently attenuated (<2.9 fold decreased), while atorvastatin and simvastatin distribution was 1.5-2.6 and 1.8-2.9 fold decreased in knockout and knockin mice.

Hepatic OATP1B1 and OATP1B3 protein levels are presented in Figure 7 (expression of all quantified transporters is summarized is supplemental Table 2). As expected, human OATP protein was not detected in wild-type mice, as well as in oatp1a/1b-knockout mice. In OATP1B1-humanized mice, hepatic expression of OATP1B1 was on average 55% lower than in human, while OATP1B3 protein was not detected. In contrast, OATP1B3 hepatic protein expression was on average 3.3 fold higher in OATP1B3-humanized mice than in human livers. As such, the relative abundance of OATP1B1 vs. OATP1B3 in these humanized mice (4.4 fold higher OATP1B3) is essentially reversed relative to the human liver, where OATP1B1 expression is higher: 1.7 fold in the present study, and on average, 2.7 fold in the literature [range = 1.1-5.1 fold] (Chu et al., 2013). These differences in hepatic OATP expression indicate that the humanized mice are likely to underestimate the importance of hepatic OATP1B1 and overestimate the contribution of OATP1B3. As such, based on these expression differences, the relative expression factor for extrapolating humanized mouse findings to humans is 2.2 for OATP1B1 and 0.30 for OATP1B3 (Hirano et al., 2004).

Discussion

The present study evaluated changes in pharmacokinetics and tissue distribution of pravastatin, atorvastatin, simvastatin (lactone and acid forms), and carboxydichlorofluorescein in oatp1a/1b-/- mice, which effectively lack hepatic oatp function (van de Steeg et al., 2010), as well as oatp1a/1b-knockout mice with liver-specific knockin of human OATP1B1 or 1B3 (van de Steeg et al., 2012). Relative to wild-type mice, systemic exposure of five different OATP substrates was markedly increased in knockout mice due to reduced clearance, volume, and/or increased bioavailability. Liver-specific knockin of human OATP1B1 or 1B3 decreased drug exposure, but not to the levels observed in wild-type mice. As such, knockin pharmacokinetic profiles were positioned between knockout and wild-type mice. Partial restoration of clearance, volume, and bioavailability in the knockins is conceptually consistent with knockout of all three major murine oatps but replacement with only one of three human OATPs (Iusuf et al., 2012b).

Since the three predominant hepatic murine oatps are absent in oatp1a/1b gene cluster knockout mice, liver distribution of substrate drugs is expected to be strikingly impaired (van de Steeg et al., 2010). In fact, liver distribution was one to two orders of magnitude decreased across the tested OATP substrates. Liver-specific knockin of human OATP1B1 or 1B3 partially restored hepatic drug distribution by up to one order of magnitude. This incomplete restoration of liver distribution in the humanized mice again emphasizes that knockin of only one of three human OATPs does not fully compensate for nearly complete loss of endogenous murine oatp function. It merits noting that unlike the liver, impaired distribution to extra-hepatic tissues was not restored in humanized mice, functionally confirming that the knockin is liver specific (van de Steeg et al., 2012).

Despite qualitative consistency in pharmacokinetic alterations in oatp1a/1b-knockout mice, the magnitude of change differed between the five analytes studied, because the disposition of these molecules is dependent on hepatic OATPs to a varying extent (Zamek-Gliszczynski et al., 2003; 2012a; Elsby et al., 2012; Shitara et al., 2013). Specifically, the relatively high magnitude of change in oral PK and liver distribution of pravastatin in oatp1a/1b-knockout mice resulted in a wide range in quantitative PK alterations. Pravastatin ($LogD_{7.4}$ = -1) is considerably more hydrophilic (lower passive permeability) than simvastatin and atorvastatin ($LogD_{7.4}$ = +1.0-1.8), thus the impact of hepatic oatp knockout on pravastatin is more pronounced. Furthermore, pravastatin exhibited the lowest oral bioavailability in wild-type mice, resulting in the greatest margin for a large-magnitude increase in oral exposure for this drug. Unlike simvastatin and atorvastatin, where intestinal metabolism is a limiting factor in oral exposure (Gertz et al., 2011) that is not subject to change by genetic OATP modification, pravastatin is not metabolized in the intestine (Varma et al., 2012). As such, pravastatin was more sensitive to the absence of hepatic OATP function than the other compounds studied.

To-date, a total of five studies of OATP substrate disposition in these knockout and transgenic models have been published, which are conceptually consistent with the current findings of altered systemic pharmacokinetics and hepatic drug distribution (van de Steeg et al., 2010; 2011; 2012; Iusuf et al., 2012a; 2013). Specifically, pravastatin, rosuvastatin, and fexofenadine were studied in oatp1a/1b-knockout mice, while paclitaxel and methotrexate disposition was examined across both knockout and OATP-humanized mice. Previously-reported alterations in pravastatin pharmacokinetics in oatp1a/1b-/- mice are quantitatively in good agreement with the present findings: intravenous exposure was increased 4 fold, oral exposure 30 fold, and liver distribution was 10-100 fold decreased (Iusuf et al., 2012a); in the

present study these changes were 4, 115, and 196 fold, respectively. Rosuvastatin intravenous exposure was 3 fold increased, oral exposure 8 fold increased, and liver distribution was decreased one order of magnitude (Iusuf et al., 2013); similarly, fexofenadine intravenous exposure was 3 fold increased and hepatic distribution 10 fold decreased (van de Steeg et al., 2010). Methotrexate intravenous exposure was 3-5 fold increased and hepatic distribution was 69-131 fold decreased (van de Steeg et al., 2010; 2011; 2013); knockin of individual human OATP isoforms partially restored methotrexate exposure (~2 fold decrease) and increased liver distribution 6-15fold (van de Steeg et al., 2013). Paclitaxel intravenous exposure was ≤2 fold increased, while liver distribution was 2-4 fold decreased (van de Steeg et al., 2011; 2013); knockin of human OATPs resulted in low and inconsistent restoration of pharmacokinetics and liver distribution, due to the relatively low overall impact of OATP on paclitaxel disposition (van de Steeg et al., 2013).

Notably murine oatps from the 1a and 1b subfamilies are also expressed in other organs relevant to drug disposition, and so attenuated statin distribution was expected in these tissues (Iusuf et al., 2012b). Evidence exists for expression of oatp1a subfamily in the renal proximal tubule (Iusuf et al., 2012b), and this was supported at a functional level in the present study by the modest decreases (1.4-2.9 fold) in atorvastatin and simvastatin kidney distribution. Quantitatively, these findings are consistent with the previously reported ≤3 fold decrease in rosuvastatin and 2 fold decrease in fexofenadine kidney distribution in oatp1a/1b-knockout mice (van de Steeg et al., 2010; Iusuf et al., 2013). Surprisingly, pravastatin renal tissue distribution was markedly increased two orders of magnitude in oatp1a/1b-knockout mice, and this increase was partially attenuated in humanized mice. Pravastatin clearance is partially renal (Singhvi et al., 1990); therefore, one possible explanation for this unexpected increase is that kidneys were

compensating for the effective absence of hepatic clearance in knockout mice. This hypothesis is supported by attenuation of the increase in knockin mice with partially restored hepatic clearance.

Oatp1a4 is an important isoform in the murine blood-brain barrier, where it contributes to brain uptake of exogenous and endogenous substrates (Kalvass et al., 2013). Previously initial uptake of four different OATP-substrate drugs was shown to be 1.3-3.8 fold impaired in oatp1a4-knockout mice during 1-minute brain perfusions (Ose et al., 2010), while fexofenadine and methotrexate *in vivo* brain distribution were 2 fold decreased (van de Steeg et al., 2010). In the present study, brain distribution of atorvastatin and simvastatin was impaired to an extent comparable with previous observations, but the magnitude of impairment in pravastatin CNS distribution (6-11 fold) was notably larger. The extent to which pravastatin appears to be taken up into the brain by OATP is greater than previously reported for a drug, and nearly approached the 19-fold enhancement in taurocholate brain uptake by Oatp1a4, the largest-magnitude functional example to-date (Ose et al., 2010). The observed increase in pravastatin brain distribution does not contradict the findings of Ose et al (2010), because 1) Ose et al. measured initial uptake in brain perfusions, where the magnitude of change is lower (Kalvass et al., 2013), and 2) Ose et al used oatp1a4-knockout as opposed to oatp1a/1b gene cluster knockout mice, in which, for example, oatp1a5 is also absent. Finally, pravastatin is far more hydrophilic than simvastatin and atorvastatin, so its lower passive CNS distribution makes the oatp1a/1b-knockout effect more apparent.

Cardiac and skeletal muscle express OATPs (ex. rodent Oatp1a4 and human OATP2B1) capable of transporting statin drugs *in vitro* (Grube et al., 2006; Sakamoto et al., 2008). Statin distribution to heart and quadriceps was up to 2.9 fold decreased in mice lacking oatp1a/1b

DMD Fast Forward. Published on November 5, 2013 as DOI: 10.1124/dmd.113.054783
This article has not been copyedited and formatted. The final version may differ from this version.

subfamilies. This trend of impaired statin muscle distribution was observed in both oatp1a/1b-knockout and OATP1B1- or OATP1B3-knockin mice, where the humanization is liver specific, such that these transgenic mice exhibit the oatp1a/1b phenotype in extrahepatic tissues (van de Steeg et al., 2012; 2013). The present study provides the first *in vivo* evidence of statin uptake into muscle by the Oatp1a/1b subfamilies. These data suggest that OATP uptake into muscle may play a role in statin myotoxicity (Neuvonen et al., 2006).

Oatp1a/1b-knockout mice are useful in qualitatively demonstrating the impact of OATPs on pharmacokinetics. The ability to quickly determine whether hepatic OATP uptake affects *in vivo* drug disposition is a major advancement in its own right. However, can these murine knockout and humanized transgenic models be used for more quantitative clinical predictions? While it is premature to claim that a preclinical-to-clinical correlation has been established based on three statins, a quantitative translational approach is proposed below and appears to be in good agreement with clinical data.

Shitara et al. (2013) estimated the contribution of OATP1B1 to human hepatic uptake to be 0.83 for pravastatin and 0.47 for atorvastatin based on pharmacokinetic changes in human carriers of OATP1B1 521T>C polymorphism(s); estimates for simvastatin are not available. Using the current preclinical data, the fractional contribution of human OATP1B1 to hepatic uptake can be estimated from the following relationship (Hirano et al., 2004; Zamek-Gliszczynski et al., 2009; 2013):

$$OATP1B1\ Hepatic\ Uptake\ Fraction = 1 - \frac{1}{\left[\left(\frac{OATP1B1\ KI\ Liver\ Kp}{oatp1a/1b\ KO\ Liver\ Kp} - 1\right) \times REF\right] + 1}$$

where OATP1B1 relative expression factor (REF) is 2.2, and the knockin (KI)/knockout (KO) Liver Kp ratio is 2.5 for pravastatin and 1.2 for atorvastatin. The fraction of hepatic uptake

mediated by human OATP1B1 is thus estimated to be 0.77 for pravastatin and 0.31 for atorvastatin, which is within 1.5 fold of estimates based on human pharmacokinetics (Shitara et al., 2013).

Elsby et al. (2012) estimated the maximal increase in statin oral exposure in the theoretical scenario of complete OATP1B1 inhibition in humans. Based on the projected maximal increase in exposure to pravastatin, atorvastatin, and simvastatin of 2.0, 3.2, and 4.8 fold (Elsby et al., 2012); the fractional contribution of OATP1B1 to overall clearance is 0.50, 0.69, and 0.79, respectively (Zamek-Gliszczynski et al., 2009). Using the current preclinical data, the fractional contribution of human OATP1B1 to oral systemic drug clearance can be estimated from the following relationship (Hirano et al., 2004; Zamek-Gliszczynski et al., 2009; 2013):

$$OATP1B1\ Oral\ Clearance\ Fraction = 1 - \frac{1}{\left[\left(\frac{oatp1a/1b\ KO\ AUCpo}{OATP1B1\ KI\ AUCpo} - 1\right) \times REF\right] + 1}$$

where OATP1B1 relative expression factor (REF) is 2.2, and the knockout (KO)/knockin (KI) oral exposure (AUCpo) ratio is 1.45, 1.39, and 3.6 for pravastatin, atorvastatin, and simvastatin, respectively. Using these data, the fractional contribution of human OATP1B1 to oral systemic drug clearance is estimated to be for 0.50, 0.46, and 0.85 for pravastatin, atorvastatin, and simvastatin, respectively, which is within 1.5 fold of human values (Elsby et al., 2012). Using these preclinical estimates, the magnitude of clinical increase in statin exposure can be predicted by the following relationship (Zamek-Gliszczynski et al., 2009; 2013):

$$Fold\ Increase\ in\ Systemic\ Exposure = \frac{1}{(1 - Fraction\ Cleared\ by\ OATP1B1)}$$

which estimates the increase in clinical exposure in the theoretical case of complete human OATP1B1 inhibition to be 2.0, 1.9, 6.8 fold for pravastatin, atorvastatin, and simvastatin, respectively, which is within 1.7 fold of human values (Elsby et al., 2012).

The proposed translational approach is only applicable to OATP hepatic uptake and its influences on systemic drug pharmacokinetics. The present study does not provide mechanistic information on translation of downstream hepatic clearance of drugs. However, the observed changes in systemic pharmacokinetics and liver distribution are consistent with OATP hepatic uptake being the rate-determining step in the removal of these drugs from circulation in mice as in humans at a gross kinetic level (Elsby et al., 2012; Shitara et al., 2013). Furthermore, accurate estimation (within 1.5 fold) of the fraction of hepatic uptake mediated by human OATP1B1 calculated based on changes in liver Kp in these mice indicates that on a gross kinetic level, the relative rate of downstream hepatic clearance is consistent with humans. Specifically, the Kp parameter is a function of uptake (modulated parameter), clearance by metabolism and/or excretion, as well as the extent of plasma and tissue binding, which are generally conserved between species (Kalvass et al., 2013). Thus, accurate prediction of the fraction of hepatic uptake mediated by human OATP1B1 calculated from changes in liver Kp in knockout versus knockin mice supports comparable relative rate of downstream clearance between mice and humans. Taken together, these two kinetic observations (OATP uptake as the rate determining step and accurate translation of liver Kp values) support the relevance of these murine models for the study of hepatic OATP uptake. However, the present and previous studies conducted in these mice provide no mechanistic characterization of downstream hepatic clearance via metabolism and/or excretion, and further validation would be needed to support studies of these processes.

In conclusion, oatp1a/1b-knockout mice are useful in determining whether hepatic OATP uptake influences systemic pharmacokinetics and hepatic distribution. In addition, they provide insight into OATP involvement in brain, kidney, and muscle drug distribution. Liver-specific knockin of OATP1B1 or OATP1B3 into these knockout mice may be used to predict the impact the on clinical pharmacokinetics, but only after correcting for the differences in protein expression in knockin mice versus humans.

Authorship Contributions

Participated in research design: Higgins, Bao, Smith, Zamek-Gliszczynski

Contributed new reagents: Fallon, Smith

Conducted experiments: Bao, Fallon

Performed data analysis: Higgins, Bao, Ke, Manro, Fallon, Smith, Zamek-Gliszczynski

Wrote or contributed to the writing of the manuscript: Higgins, Bao, Ke, Manro, Fallon, Smith Zamek-Gliszczynski

References:

Badolo L, Rasmussen LM, Hansen HR, and Sveigaard C (2010) Screening of OATP1B1/3 and OCT1 inhibitors in cryopreserved hepatocytes in suspension. *European journal of pharmaceutical sciences : official journal of the European Federation for Pharmaceutical Sciences* **40:**282-288.

Balogh LM, Kimoto E, Chupka J, Zhang H, and Lai Y (2012) Membrane Protein Quantification by Peptide-Based Mass Spectrometry Approaches: Studies on the Organic Anion-Transporting Polypeptide Family. *J Proteomics Bioinform* **S4** 003.

Chen C, Stock JL, Liu X, Shi J, Van Deusen JW, DiMattia DA, Dullea RG, and de Morais SM (2008) Utility of a novel Oatp1b2 knockout mouse model for evaluating the role of Oatp1b2 in the hepatic uptake of model compounds. *Drug metabolism and disposition: the biological fate of chemicals* **36:**1840-1845.

Chu X, Bleasby K, and Evers R (2013) Species differences in drug transporters and implications for translating preclinical findings to humans. *Expert opinion on drug metabolism & toxicology* **9:**237-252.

Elsby R, Hilgendorf C, and Fenner K (2012) Understanding the critical disposition pathways of statins to assess drug-drug interaction risk during drug development: it's not just about OATP1B1. *Clinical pharmacology and therapeutics* **92:**584-598.

Fallon JK, Neubert H, Hyland R, Goosen TC, and Smith PC (2013) Targeted Quantitative Proteomics for the Analysis of 14 UGT1As and -2Bs in Human Liver using nanoUPLC-MS/MS with Selected Reaction Monitoring. *Journal of proteome research*.

Gertz M, Houston JB, and Galetin A (2011) Physiologically based pharmacokinetic modeling of intestinal first-pass metabolism of CYP3A substrates with high intestinal extraction. *Drug metabolism and disposition: the biological fate of chemicals* **39:**1633-1642.

Giacomini KM, Balimane PV, Cho SK, Eadon M, Edeki T, Hillgren KM, Huang SM, Sugiyama Y, Weitz D, Wen Y, Xia CQ, Yee SW, Zimdahl H, and Niemi M (2013) International Transporter Consortium commentary on clinically important transporter polymorphisms. *Clinical pharmacology and therapeutics* **94:**23-26.

Giacomini KM, Huang SM, Tweedie DJ, Benet LZ, Brouwer KL, Chu X, Dahlin A, Evers R, Fischer V, Hillgren KM, Hoffmaster KA, Ishikawa T, Keppler D, Kim RB, Lee CA, Niemi M, Polli JW, Sugiyama Y, Swaan PW, Ware JA, Wright SH, Yee SW, Zamek-Gliszczynski MJ, and Zhang L (2010) Membrane transporters in drug development. *Nature reviews Drug discovery* **9:**215-236.

Grube M, Kock K, Oswald S, Draber K, Meissner K, Eckel L, Bohm M, Felix SB, Vogelgesang S, Jedlitschky G, Siegmund W, Warzok R, and Kroemer HK (2006) Organic anion transporting polypeptide 2B1 is a high-affinity transporter for atorvastatin and is expressed in the human heart. *Clinical pharmacology and therapeutics* **80:**607-620.

Hirano M, Maeda K, Shitara Y, and Sugiyama Y (2004) Contribution of OATP2 (OATP1B1) and OATP8 (OATP1B3) to the hepatic uptake of pitavastatin in humans. *The Journal of pharmacology and experimental therapeutics* **311:**139-146.

Iusuf D, Sparidans RW, van Esch A, Hobbs M, Kenworthy KE, van de Steeg E, Wagenaar E, Beijnen JH, and Schinkel AH (2012a) Organic anion-transporting polypeptides 1a/1b control the hepatic uptake of pravastatin in mice. *Molecular pharmaceutics* **9:**2497-2504.

Iusuf D, van de Steeg E, and Schinkel AH (2012b) Functions of OATP1A and 1B transporters in vivo: insights from mouse models. *Trends Pharmacol Sci* **33:**100-108.

Iusuf D, van Esch A, Hobbs M, Taylor M, Kenworthy KE, van de Steeg E, Wagenaar E, and Schinkel AH (2013) Murine Oatp1a/1b uptake transporters control rosuvastatin systemic exposure without affecting its apparent liver exposure. *Molecular pharmacology* **83:**919-929.

Ji C, Tschantz WR, Pfeifer ND, Ullah M, and Sadagopan N (2012) Development of a multiplex UPLC-MRM MS method for quantification of human membrane transport proteins OATP1B1, OATP1B3 and OATP2B1 in in vitro systems and tissues. *Analytica chimica acta* **717:**67-76.

Kalvass JC, Polli JW, Bourdet DL, Feng B, Huang SM, Liu X, Smith QR, Zhang LK, and Zamek-Gliszczynski MJ (2013) Why clinical modulation of efflux transport at the human blood-brain barrier is unlikely: the ITC evidence-based position. *Clinical pharmacology and therapeutics* **94:**80-94.

Neuvonen PJ, Niemi M, and Backman JT (2006) Drug interactions with lipid-lowering drugs: mechanisms and clinical relevance. *Clinical pharmacology and therapeutics* **80:**565-581.

Niemi M (2007) Role of OATP transporters in the disposition of drugs. *Pharmacogenomics* **8:**787-802.

Ohtsuki S, Uchida Y, Kubo Y, and Terasaki T (2011) Quantitative targeted absolute proteomics-based ADME research as a new path to drug discovery and development: methodology, advantages, strategy, and prospects. *Journal of pharmaceutical sciences* **100:**3547-3559.

Ose A, Kusuhara H, Endo C, Tohyama K, Miyajima M, Kitamura S, and Sugiyama Y (2010) Functional characterization of mouse organic anion transporting peptide 1a4 in the uptake

and efflux of drugs across the blood-brain barrier. *Drug metabolism and disposition: the biological fate of chemicals* **38:**168-176.

Picotti P, Rinner O, Stallmach R, Dautel F, Farrah T, Domon B, Wenschuh H, and Aebersold R (2010) High-throughput generation of selected reaction-monitoring assays for proteins and proteomes. *Nature methods* **7:**43-46.

Sakamoto K, Mikami H, and Kimura J (2008) Involvement of organic anion transporting polypeptides in the toxicity of hydrophilic pravastatin and lipophilic fluvastatin in rat skeletal myofibres. *British journal of pharmacology* **154:**1482-1490.

Shitara Y, Maeda K, Ikejiri K, Yoshida K, Horie T, and Sugiyama Y (2013) Clinical significance of organic anion transporting polypeptides (OATPs) in drug disposition: their roles in hepatic clearance and intestinal absorption. *Biopharmaceutics & drug disposition* **34:**45-78.

Singhvi SM, Pan HY, Morrison RA, and Willard DA (1990) Disposition of pravastatin sodium, a tissue-selective HMG-CoA reductase inhibitor, in healthy subjects. *British journal of clinical pharmacology* **29:**239-243.

van de Steeg E, Stranecky V, Hartmannova H, Noskova L, Hrebicek M, Wagenaar E, van Esch A, de Waart DR, Oude Elferink RP, Kenworthy KE, Sticova E, al-Edreesi M, Knisely AS, Kmoch S, Jirsa M, and Schinkel AH (2012) Complete OATP1B1 and OATP1B3 deficiency causes human Rotor syndrome by interrupting conjugated bilirubin reuptake into the liver. *The Journal of clinical investigation* **122:**519-528.

van de Steeg E, van der Kruijssen CM, Wagenaar E, Burggraaff JE, Mesman E, Kenworthy KE, and Schinkel AH (2009) Methotrexate pharmacokinetics in transgenic mice with liver-

specific expression of human organic anion-transporting polypeptide 1B1 (SLCO1B1). *Drug metabolism and disposition: the biological fate of chemicals* **37:**277-281.

van de Steeg E, van Esch A, Wagenaar E, Kenworthy KE, and Schinkel AH (2013) Influence of human OATP1B1, OATP1B3, and OATP1A2 on the pharmacokinetics of methotrexate and paclitaxel in humanized transgenic mice. *Clinical cancer research : an official journal of the American Association for Cancer Research* **19:**821-832.

van de Steeg E, van Esch A, Wagenaar E, van der Kruijssen CM, van Tellingen O, Kenworthy KE, and Schinkel AH (2011) High impact of Oatp1a/1b transporters on in vivo disposition of the hydrophobic anticancer drug paclitaxel. *Clinical cancer research : an official journal of the American Association for Cancer Research* **17:**294-301.

van de Steeg E, Wagenaar E, van der Kruijssen CM, Burggraaff JE, de Waart DR, Elferink RP, Kenworthy KE, and Schinkel AH (2010) Organic anion transporting polypeptide 1a/1b-knockout mice provide insights into hepatic handling of bilirubin, bile acids, and drugs. *The Journal of clinical investigation* **120:**2942-2952.

van Montfoort JE, Hagenbuch B, Groothuis GM, Koepsell H, Meier PJ, and Meijer DK (2003) Drug uptake systems in liver and kidney. *Current drug metabolism* **4:**185-211.

Varma MV, Lai Y, Feng B, Litchfield J, Goosen TC, and Bergman A (2012) Physiologically based modeling of pravastatin transporter-mediated hepatobiliary disposition and drug-drug interactions. *Pharmaceutical research* **29:**2860-2873.

Yang AY, Sun L, Musson DG, and Zhao JJ (2005) Application of a novel ultra-low elution volume 96-well solid-phase extraction method to the LC/MS/MS determination of simvastatin and simvastatin acid in human plasma. *J Pharm Biomed Anal* **38:**521-527.

Zaher H, Meyer zu Schwabedissen HE, Tirona RG, Cox ML, Obert LA, Agrawal N, Palandra J, Stock JL, Kim RB, and Ware JA (2008) Targeted disruption of murine organic anion-transporting polypeptide 1b2 (Oatp1b2/Slco1b2) significantly alters disposition of prototypical drug substrates pravastatin and rifampin. *Molecular pharmacology* **74:**320-329.

Zamek-Gliszczynski MJ, Bedwell DW, Bao JQ, and Higgins JW (2012a) Characterization of SAGE Mdr1a (P-gp), Bcrp, and Mrp2 knockout rats using loperamide, paclitaxel, sulfasalazine, and carboxydichlorofluorescein pharmacokinetics. *Drug metabolism and disposition: the biological fate of chemicals* **40:**1825-1833.

Zamek-Gliszczynski MJ, Hoffmaster KA, Tweedie DJ, Giacomini KM, and Hillgren KM (2012b) Highlights from the International Transporter Consortium second workshop. *Clinical pharmacology and therapeutics* **92:**553-556.

Zamek-Gliszczynski MJ, Kalvass JC, Pollack GM, and Brouwer KL (2009) Relationship between drug/metabolite exposure and impairment of excretory transport function. *Drug metabolism and disposition: the biological fate of chemicals* **37:**386-390.

Zamek-Gliszczynski MJ, Lee CA, Poirier A, Bentz J, Chu X, Ellens H, Ishikawa T, Jamei M, Kalvass JC, Nagar S, Pang KS, Korzekwa K, Swaan PW, Taub ME, Zhao P, and Galetin A (2013) ITC Recommendations for Transporter Kinetic Parameter Estimation and Translational Modeling of Transport-Mediated PK and DDIs in Humans. *Clinical pharmacology and therapeutics* **94:**64-79.

Zamek-Gliszczynski MJ, Xiong H, Patel NJ, Turncliff RZ, Pollack GM, and Brouwer KL (2003) Pharmacokinetics of 5 (and 6)-carboxy-2',7'-dichlorofluorescein and its diacetate

promoiety in the liver. *The Journal of pharmacology and experimental therapeutics* **304:**801-809.

Figure Legends:

Figure 1. Carboxydichlorofluorescein concentration-time profiles following administration of a 10 mg/kg intravenous bolus dose (A and B) to wild-type (closed circles), oatp1a/1b-knockout (open circles), OATP1B1-knockin (red triangles), or OATP1B3-knockin (red squares) mice. Comparison of oatp1a/1b-knockout to wild-type mice is presented in panel A. OATP1B1- and OATP1B3-knockin mice are displayed in red relative to mean pharmacokinetic profiles for wild-type (black solid line) and oatp1a/1b-knockout (black dashed line) mice in panel B. Mean + S.D., n = 10. Carboxydiclorofluorescein liver-to-blood concentration ratio determined at 6 hours post intravenous administration (C). Mean + S.D., n = 4. *$p < 0.05$, knockout or knockin vs. wild-type mice.

Figure 2. Pravastatin concentration-time profiles following administration of a 10 mg/kg intravenous bolus dose (A and B) or a 100 mg/kg oral dose (C and D) to wild-type (closed circles), oatp1a/1b-knockout (open circles), OATP1B1-knockin (red triangles), or OATP1B3-knockin (red squares) mice. Comparison of oatp1a/1b-knockout to wild-type mice is presented in panels A and C. OATP1B1- and OATP1B3-knockin mice are displayed in red relative to mean pharmacokinetic profiles for wild-type (black solid line) and oatp1a/1b-knockout (black dashed line) mice in panels B and D. Mean + S.D., n = 4.

Figure 3. Atorvastatin concentration-time profiles following administration of a 10 mg/kg intravenous bolus dose (A and B) or a 300 mg/kg oral dose (C and D) to wild-type (closed circles), oatp1a/1b-knockout (open circles), OATP1B1-knockin (red triangles), or OATP1B3-knockin (red squares) mice. Comparison of oatp1a/1b-knockout to wild-type mice is presented

in panels A and C. OATP1B1- and OATP1B3-knockin mice are displayed in red relative to mean pharmacokinetic profiles for wild-type (black solid line) and oatp1a/1b-knockout (black dashed line) mice in panels B and D. Mean + S.D., n = 5-6. *$p < 0.05$ knockout or knockin vs. wild type mice.

Figure 4. Simvastatin lactone composite concentration-time profiles following administration of a 10 mg/kg intravenous bolus dose (A and B) or a 100 mg/kg oral dose (C and D) to wild-type (closed circles), oatp1a/1b-knockout (open circles), OATP1B1-knockin (red triangles), or OATP1B3-knockin (red squares) mice. Comparison of oatp1a/1b-knockout to wild-type mice is presented in panels A and C. OATP1B1- and OATP1B3-knockin mice are displayed in red relative to mean pharmacokinetic profiles for wild-type (black solid line) and oatp1a/1b-knockout (black dashed line) mice in panels B and D. Mean + S.D., n = 5-6 mice per time point.

Figure 5. Simvastatin acid composite concentration-time profiles following administration of a 10 mg/kg intravenous bolus dose (A and B) or a 100 mg/kg oral dose (C and D) of simvastatin lactone to wild-type (closed circles), oatp1a/1b-knockout (open circles), OATP1B1-knockin (red triangles), or OATP1B3-knockin (red squares) mice. Comparison of oatp1a/1b-knockout to wild-type mice is presented in panels A and C. OATP1B1- and OATP1B3-knockin mice are displayed in red relative to mean pharmacokinetic profiles for wild-type (black solid line) and oatp1a/1b-knockout (black dashed line) mice in panels B and D. Mean + S.D., n = 5-6 mice per time point.

Figure 6. Pravastatin (A), atorvastatin (B), and simvastatin (C) tissue distribution in wild-type, oatp1a/1b-knockout, OATP1B1- or OATP1B3-knockin mice. Pravastatin and atorvastatin tissue-to-blood concentration ratios were measured 6 hours following oral administration of a 100 mg/kg oral dose. Total simvastatin (lactone + acid) tissue-to-plasma concentration ratios were measured at 5 and 6 hours following oral administration of a 100 mg/kg oral simvastatin lactone dose. Mean + S.D., n = 3-6 (pravastatin and atorvastatin) and 11-12 (simvastatin). *$p < 0.05$, knockout or knockin vs. wild-type mice.

Figure 7. OATP1B1 and OATP1B3 protein expression in wild-type, oatp1a/1b-knockout, OATP1B1- or OATP1B3-knockin mouse and human livers. Mean + S.D., n = 4 mouse and 8 human livers. *$p < 0.05$, knockin mouse vs. human liver OATP1B1 or OATP1B3 protein expression.

DMD Fast Forward. Published on November 5, 2013 as DOI: 10.1124/dmd.113.054783
This article has not been copyedited and formatted. The final version may differ from this version.

Table 1: Pharmacokinetic parameters.

Parameter	Wild Type	oatp1a/1b KO	OATP1B1 KI	OATP1B3 KI
Carboxydichlorofluorescein (10 mg/kg IV; Mean ± S.D., n = 10)				
AUC (μg·h/mL)[b]	22.2 ± 17.6	57.0 ± 64.0*	35.8 ± 24.7	21.8 ± 6.9
CL_{blood} (mL/min/kg)	10.1 ± 4.0	5.8 ± 3.6*	5.8 ± 2.0*	8.2 ± 2.1
$V_{D,SS}$ (mL/kg)	583 ± 419	264 ± 144	237 ± 97	327 ± 78
Pravastatin (10 mg/kg IV; Mean ± S.D., n = 4)				
AUC (μg·h/mL)	13.7 ± 9.6	58.8 ± 92.8	12.8 ± 1.8	50.0 ± 56.5
CL_{blood} (mL/min/kg)	15.8 ± 7.4	10.6 ± 7.0	13.2 ± 1.8	8.1 ± 6.8
$V_{D,SS}$ (mL/kg)	265 ± 101	210 ± 96	227 ± 100	182 ± 75
Pravastatin (100 mg/kg PO; Mean ± S.D., n = 4)				
AUC (μg·h/mL)	0.21 ± 0.04	24.1 ± 4.8*	16.6 ± 1.4*	15.3 ± 2.7*
Cmax (ng/mL)	91 ± 34	19,400 ± 9,530*	11,600 ± 8,240*	10,300 ± 6,170*
Tmax (h)	1.8 ± 2.8	0.6 ± 0.3	0.6 ± 0.3	0.6 ± 0.3
F (%)	0.2 ± 0.1	14.7 ± 10.9*	13.2 ± 2.5*	7.6 ± 6.1*
Atorvastatin (10 mg/kg IV; Mean ± S.D., n = 6)				
AUC (μg·h/mL)	5.2 ± 3.4	89.1 ± 161.1*	16.7 ± 28.5	7.9 ± 4.2
CL_{blood} (mL/min/kg)	48 ± 32	12 ± 10*	29 ± 16	27 ± 13
$V_{D,SS}$ (mL/kg)	816 ± 285	323 ± 199*	475 ± 219	404 ± 162
Atorvastatin (300 mg/kg PO; Mean ± S.D., n = 5-6)				
AUC (μg·h/mL)	4.9 ± 8.2	14.4 ± 6.4*	10.4 ± 4.4*	96.4 ± 5.9*
Cmax (ng/mL)	2,160 ± 3,110	8,778 ± 4,763*	6,762 ± 3,140*	6,407 ± 3,973*
Tmax (h)	3.0 ± 2.3	0.6 ± 0.3*	0.8 ± 0.3*	1.5 ± 2.2
F (%)	3.2 ± 3.4	2.1 ± 2.0	6.8 ± 3.4	4.5 ± 3.3
Simvastatin (10 mg/kg IV; Composite PK mean, n = 5-6 mice per time point)				
Lactone AUC (μg·h/mL)	2.04	3.32	3.86	2.43
Acid AUC (μg·h/mL)	1.55	2.87	3.91	2.04
Lactone CL(mL/min/kg)	81.7	50.2	43.2	68.6
Total CL (mL/min/kg)[a]	47.3	27.5	21.9	38.0
$V_{D,SS}$ (mL/kg)	13,900	11,900	12,500	12,500
Simvastatin (100 mg/kg PO; Composite PK mean, n = 5-6 mice per time point)				
Lactone AUC (μg·h/mL)	3.87	8.24	2.85	4.32
Acid AUC (μg·h/mL)	3.17	10.3	2.58	11.4
Lactone Cmax (ng/mL)	1,640	1,610	517	767
Acid Cmax (ng/mL)	1,360	1,270	430	679
Lactone Tmax (h)	1.0	1.0	1.0	1.5
Acid Tmax (h)	1.0	1.0	1.0	1.5
Lactone F (%)	19.0	24.8	7.4	17.8
Total F (%)[a]	19.6	29.8	7.0	34.8

[a]Total simvastatin is the sum of lactone and acid normalized for molecular weight difference
[b]AUC values for carboxydiclorofluorescein and simvastatin are extrapolated to infinity; AUC values for pravastatin and atorvastatin are reported through the last time point due to inability to estimate terminal slope in some animal groups (see Figures 2-3).
*$p < 0.05$, knockout or knockin vs. wild-type mice.

DMD Fast Forward. Published on November 5, 2013 as DOI: 10.1124/dmd.113.054783
This article has not been copyedited and formatted. The final version may differ from this version.

Figure 1.

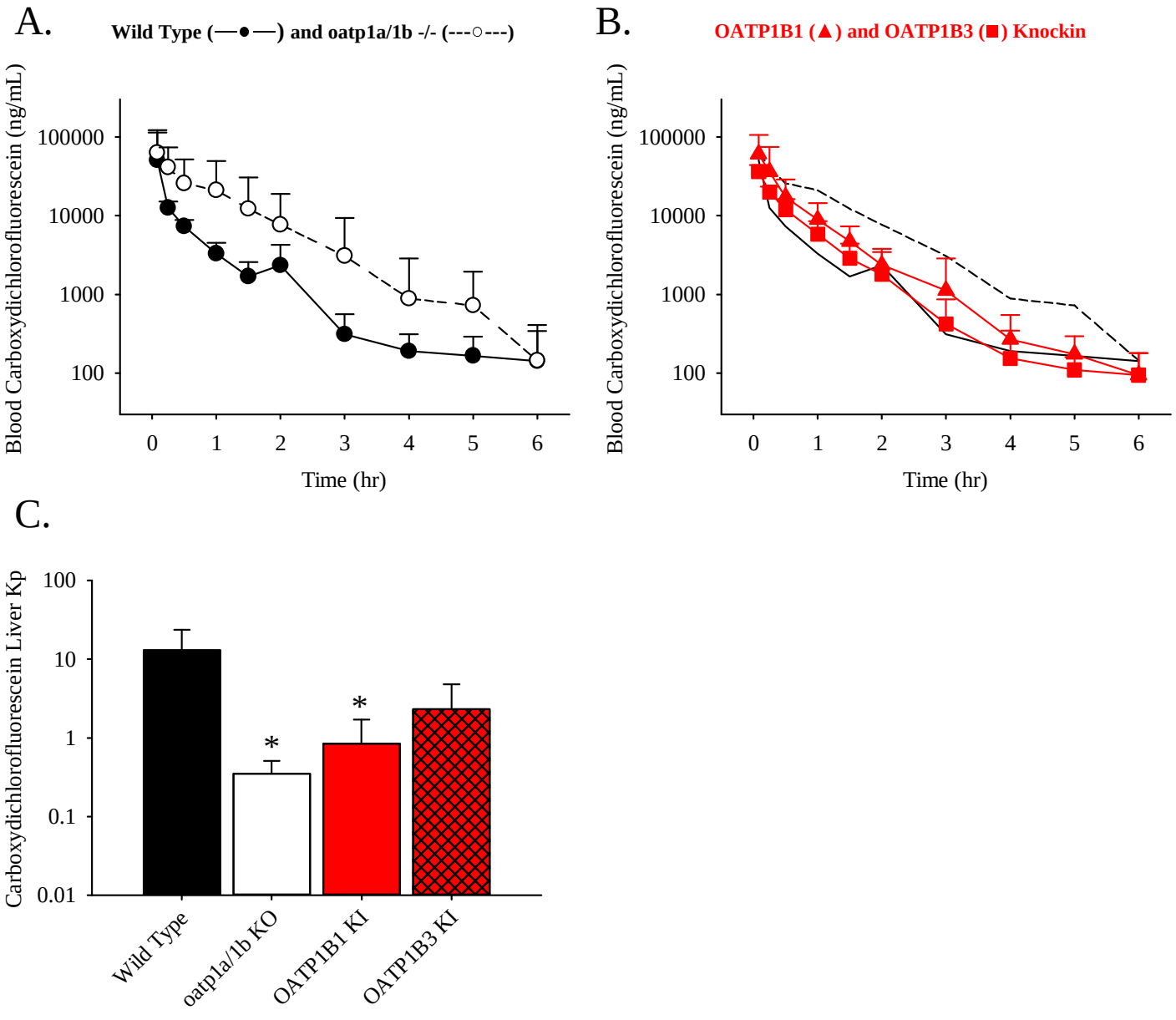

DMD Fast Forward. Published on November 5, 2013 as DOI: 10.1124/dmd.113.054783
This article has not been copyedited and formatted. The final version may differ from this version.

Figure 2.

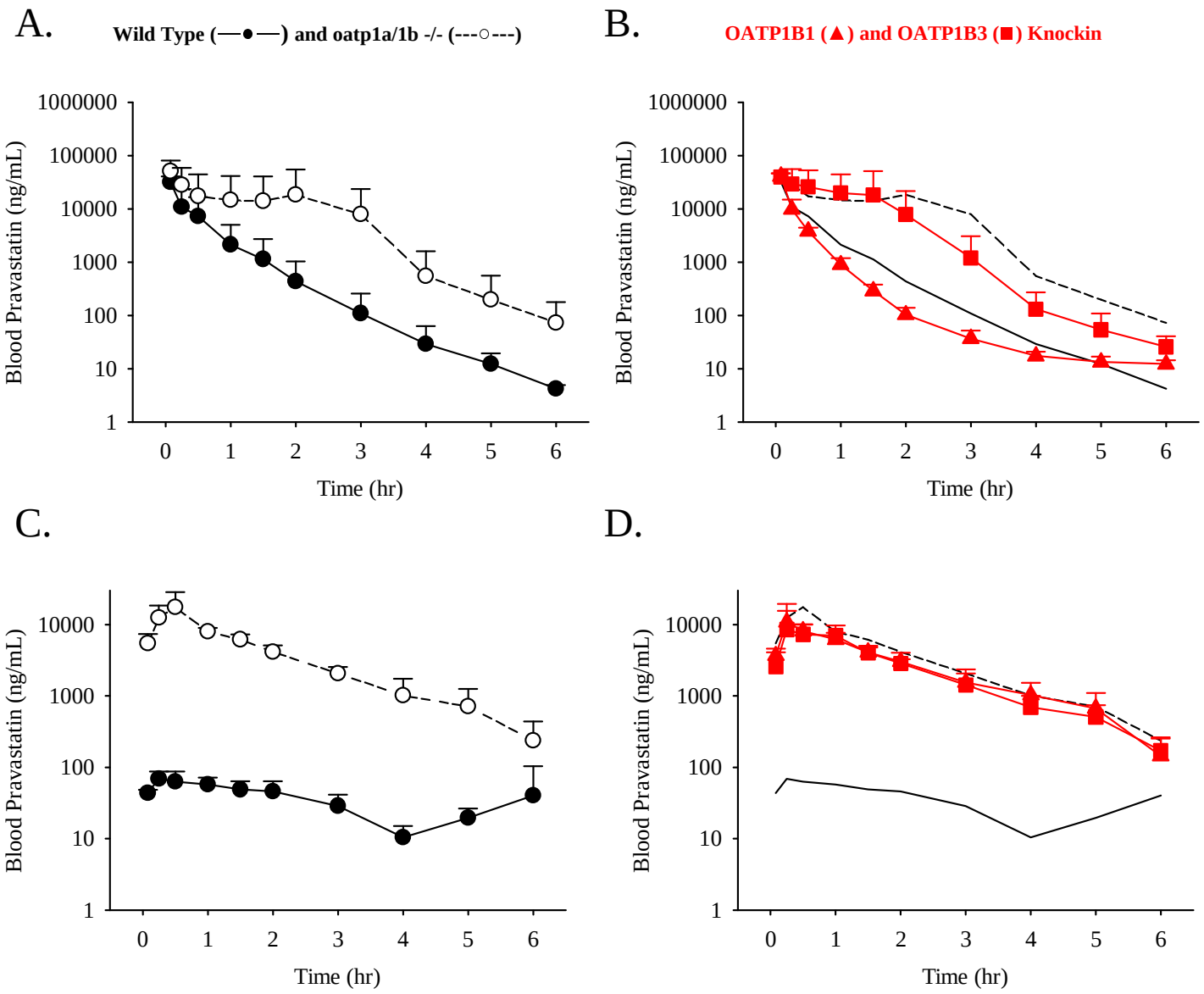

DMD Fast Forward. Published on November 5, 2013 as DOI: 10.1124/dmd.113.054783
This article has not been copyedited and formatted. The final version may differ from this version.

Figure 3.

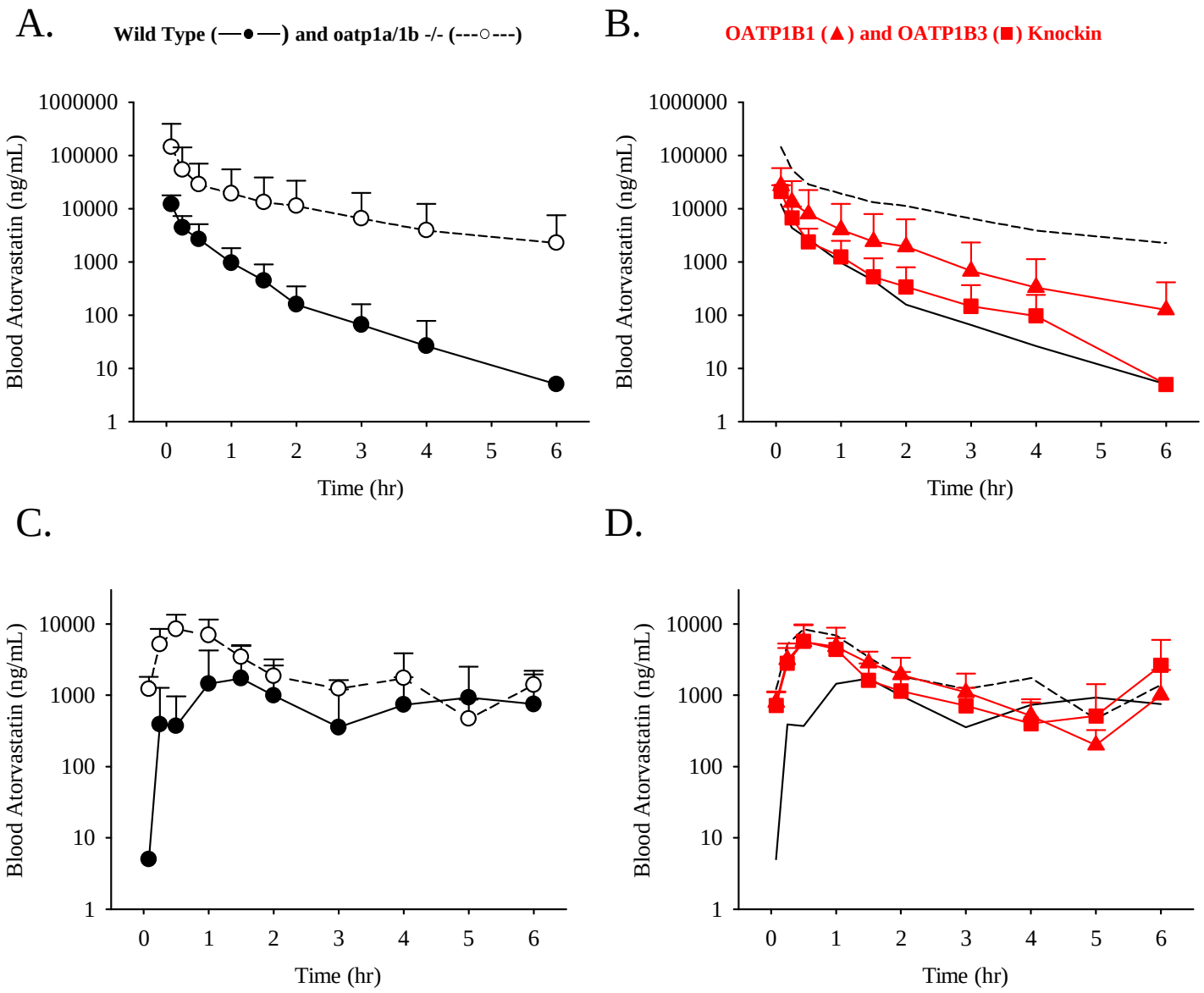

DMD Fast Forward. Published on November 5, 2013 as DOI: 10.1124/dmd.113.054783
This article has not been copyedited and formatted. The final version may differ from this version.

Figure 4.

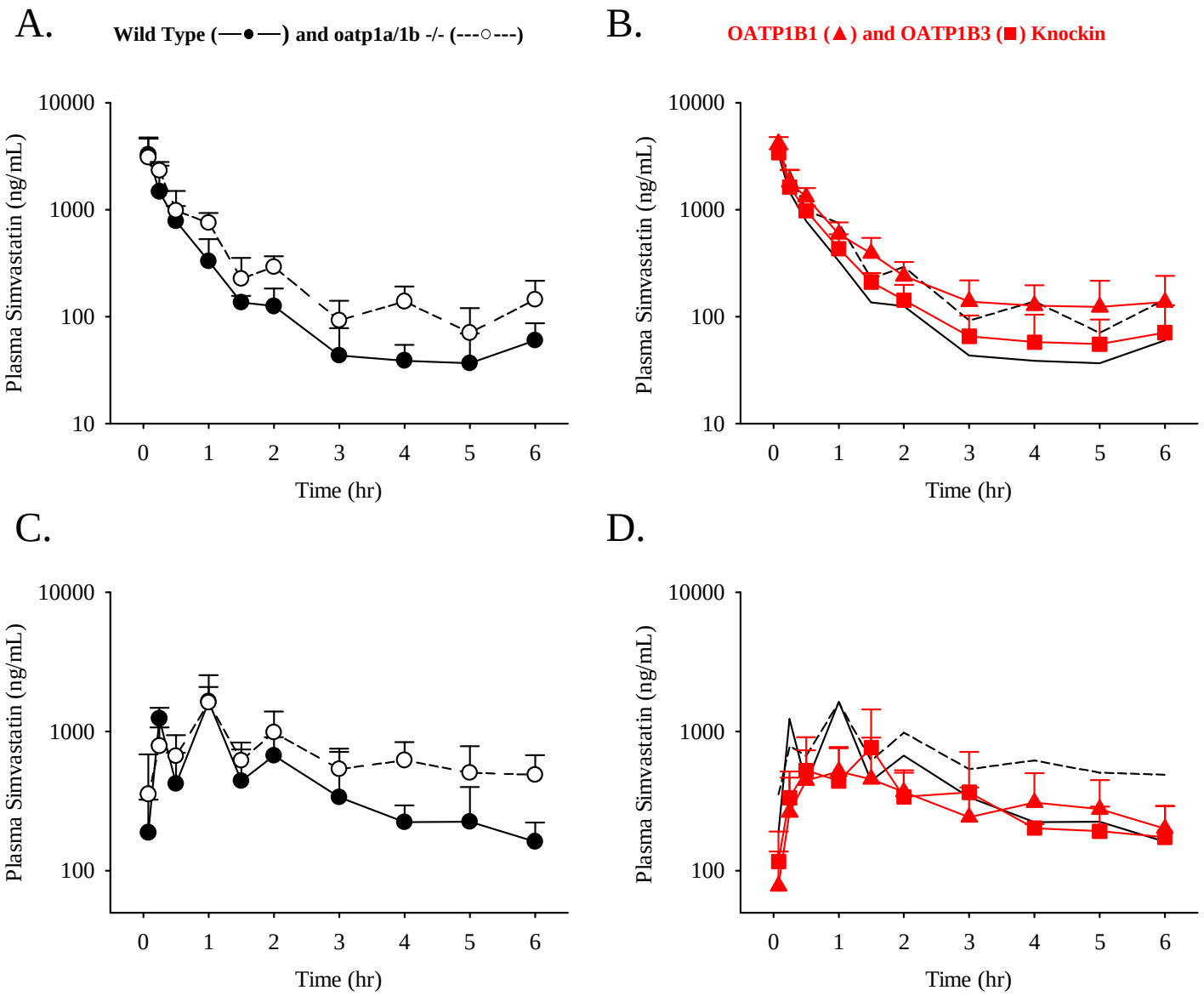

DMD Fast Forward. Published on November 5, 2013 as DOI: 10.1124/dmd.113.054783
This article has not been copyedited and formatted. The final version may differ from this version.

Figure 5.

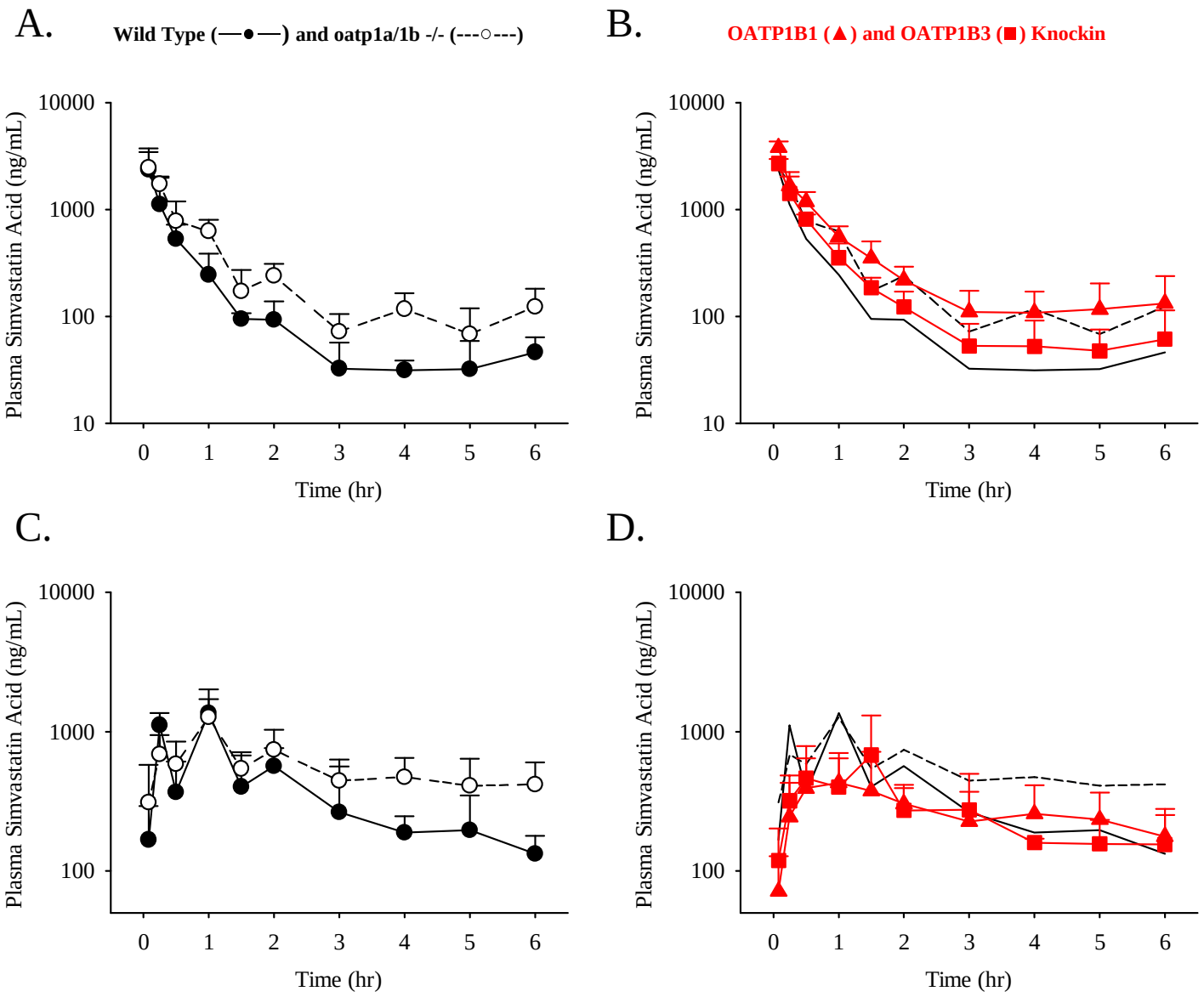

DMD Fast Forward. Published on November 5, 2013 as DOI: 10.1124/dmd.113.054783
This article has not been copyedited and formatted. The final version may differ from this version.

Figure 6.

A.

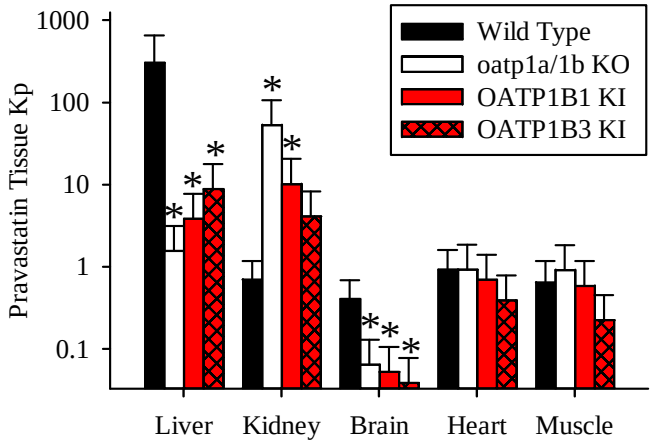

B.

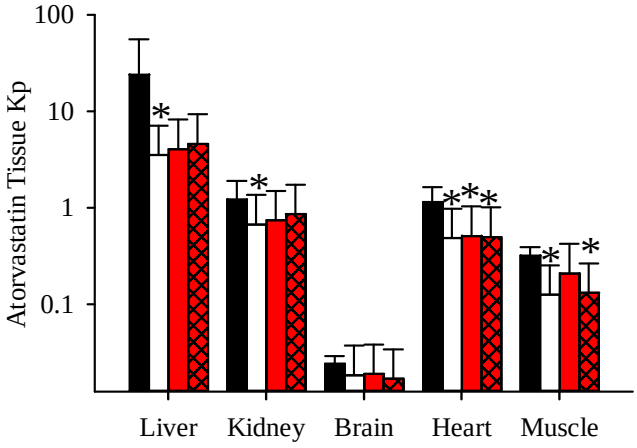

C.

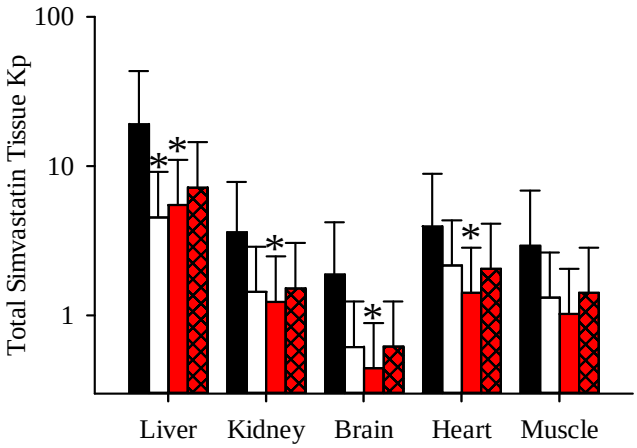

DMD Fast Forward. Published on November 5, 2013 as DOI: 10.1124/dmd.113.054783
This article has not been copyedited and formatted. The final version may differ from this version.

Figure 7.